ROYAL SOCIETY OF CHEMISTRY

PCCP

Influence of Side Chain Isomerism on the Rigidity of Poly(3-alkylthiophenes) in Solutions Revealed by Neutron Scattering

Complete List of Authors:	Hong, William; Oak Ridge National Laboratory, Neutron Scattering Division Lam, Christopher; Oak Ridge National Laboratory, Neutron Scattering Division Wang, Yangyang; Oak Ridge National Laboratory, Center for Nanophase Materials Sciences He, Youjun; ORNL, Sánchez-Díaz, Luis; Oak Ridge National Laboratory, Neutron Scattering Division Do, Changwoo; Oak Ridge National Laboratory, Neutron Scattering Division Chen, Wei-Ren; Oak Ridge National Laboratory, Neutron Scattering Division

SCHOLARONE™
Manuscripts

Journal Name

COMMUNICATION

Please do not adjust margins

Influence of Side Chain Isomerism on the Rigidity of Poly(3-alkylthiophenes) in Solutions Revealed by Neutron Scattering

William D. Hong[a], Christopher N. Lam[a], Yangyang Wang[b], Youjun He[b], Luis E. Sánchez-Díaz[a], Changwoo Do[a], and Wei-Ren Chen[ac]*

Using small-angle neutron scattering, we conducted a detailed conformational study of poly(3-alkylthiophene) solutions in deuterated dicholorobenzene. The focus was placed on addressing the influence of spatial arrangement of side chain constituents on backbone conformation. We demonstrate that by introducing a branch point in the side chain, side chain steric interactions may promote torsional motion between backbone units, resulting in greater chain flexibility. Our findings highlight the key role of topological isomerism in determining the chain rigidity and shine new light on the debate about the effective approaches for optimizing the electronic properties of conducting polymers via side chain engineering.

Conjugated polymers are synthetic macromolecules that are characterized by a backbone consisting of alternating double and single bonds.[1-4] This conjugated structure provides overlapping p-orbitals for delocalised π-electrons and allows them to be electrically conducting upon appropriate doping.[5] Conjugated polymers are found in a variety of applications.[6-11] The most exploited one is their use as organic electronics including photovoltaic cells and organic field-effect transistors[12-17]; they are also proposed for many other applications, such as in the molecular imaging[18] and pharmaceutical fields[19].

By incorporating soluble side chains into the backbone, one can increase the solubility of conjugated polymers in common organic solvents to facilitate their processing.[20-21] Among all the developed solution-processable conjugated polymers, poly(3-alkylthiophenes) (P3ATs) represent one of the most studied systems because of its exceptional chemical stability, mechanical strength, and optoelectronic properties.[22-24] A direct connection between the chain conformations of P3ATs in their solution states and optoelectronic properties in bulk has been recognized.[9,25,26] Unlike traditional flexible polymers, which can be described as random coils when dissolved in solution,[27] conjugated polymers are characterized by more stiff conformations due to the side chain steric interactions between

the neighbouring monomers and strong inter chain interactions.[9,28] The prospect of optimizing the electronic properties of P3ATs by controlling their conformation has motivated a series of scattering studies to investigate the structural origin of backbone stiffness.[29-37] Multiple factors, including molecular weight and its distributions, side chain structures, regioregularity, and backbone defects, have been demonstrated to hinder the chain free rotation and contribute to the chain stiffness of P3ATs.

One intriguing aspect of tuning backbone conformation is through varying side chain isomerism. The difference in the spatial arrangement of side chain constituents in a thiophene unit is expected to change the interactions between neighbouring monomers and surroundings. The critical question of how the molecular stiffness of P3ATs depends on the structural isomerism of their side chain has not been answered. Motivated by this challenge, in this report we used small-angle neutron scattering (SANS) to investigate the influence of side chain molecular structure on the backbone conformation of two P3AT systems, the commonly studied poly(3-hexylthiophene) (P3HT) and poly(3-(4'-methylpentyl) thiophene) (P3(4MP)T), respectively. As indicated by the insets of Figure 1, they have the same chemical formula but different structures. One common parameter to quantify the molecular stiffness is the persistence length, which separates the small length scales below which the chain is viewed as a stiff rod and the large scales over which a chain takes the shape of a random walk with a unit step of size b. By analysing the SANS spectra measured from solutions of P3HT and P3(4MP)T, we demonstrate that P3(4MP)T clearly has a smaller Kuhn segment length b than that of P3HT under the same conditions.
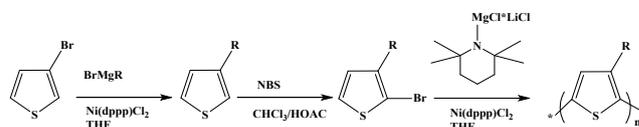
Scheme 1. Scheme illustrating the synthesis of P3HT and P3(4MP)T.

---

a. Neutron Scattering Division, Oak Ridge National Laboratory, Oak Ridge, Tennessee 37831, USA.
b. Center for Nanophase Materials Sciences, Oak Ridge National Laboratory, Oak Ridge, Tennessee 37831, USA.
c. Jülich Centre for Neutron Science, Forschungszentrum Jülich GmbH, Outstation at SNS, Oak Ridge National Laboratory, Oak Ridge, TN 37831, USA.

P3HT and P3(4MP)T were synthesized at the Center for Nanophase Materials Sciences (CNMS), Oak Ridge National Laboratory (ORNL), by a modified GRIM method.[38,39] The synthetic route is shown in Scheme 1. Briefly, in an inert gas environment, 3-bromothiophene and alkyl magnesium bromide react via a Kumada reaction[40] with Ni(dppp)Cl$_2$ as the catalyst to yield 3-alkylthiophene compounds. After reacting with NBS, 2-bromo-3-alkythiophene monomers were obtained. These monomers were polymerized with a Grignard reagent (2, 2, 6, 6-tetramethylpiperidinyl magnesium chloride lithium chloride complex solution) using Ni(dppp)Cl$_2$ as the catalyst. The final polymers were purified by multiple extractions. Both polymers are characterized by ^{1}H-NMR, indicating their very high regioregularity (>97%). From size exclusion chromatography (SEC) in chloroform, calibrated using a PS standard, the apparent average molecular weights of P3HT and P3(4MP)T are found to be 18.4 kg/mol and 33.0 kg/mol, respectively, with dispersity values of Đ = 1.09 and 1.13, respectively. Both polymers were further characterized by UV-Vis.
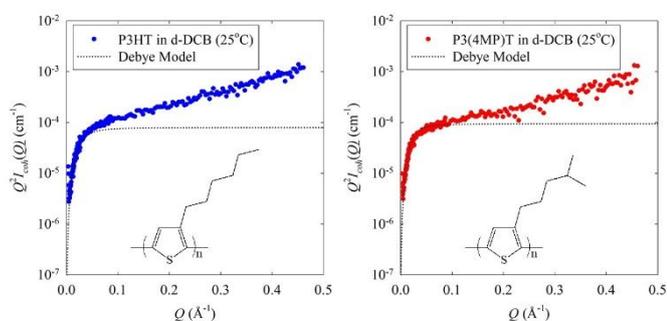
Figure 1. The Kratky plots of SANS coherent intensities of P3HT (left panel) and P3(4MP)T (right panel) in d-DCB. The molecular structures of conjugated polymers are given in the insets.

SANS measurements were carried out at the Extended Q-Range Small-Angle Neutron Scattering Diffractometer (EQ-SANS) at the Spallation Neutron Source (SNS), ORNL. The scattering wavevector Q ranged from 0.005 to 0.5 Å^{-1}. The samples were contained in Hellma quartz cells with a 2 mm path length. The measured data were corrected for detector background, sensitivity, and scattering contributions from the empty cells. The intensities were normalized to absolute units using the reference scattering from a calibrated standard. Dilute solutions of P3HT and P3(4MP)T were prepared in o-dicholorbenzene-d4 (d-DCB) at a concentration of 2 mg/mL to minimize the contributions from inter-chain spatial correlation to the collected SANS signal. The solutions were kept at 35 °C overnight under inert atmosphere.

Before presenting the quantitative conformational characteristics obtained from SANS data analysis, it is instructive to investigate the qualitative features of the SANS spectra: Figure 1 shows the Kratky plots of the SANS coherent intensities of P3HT (left panel) and P3(4MP)T (right panel) in deuterated dichlorobenzene (d-DCB). In this representation, the molecular swelling of P3HT and P3(4MP)T conjugated polymers are revealed by the high-Q upturn in the experimental

results (coloured symbols) that deviate from the predicted plateau of the Debye model (dotted curves).[41] This observed non-Gaussian conformational feature is possibly due to the excluded volume interactions of the polymers in d-DCB. In Figure 2 we present the SANS absolute intensities $I(Q)$ obtained from the d-DCB solutions of P3HT (blue symbols) and P3(4MP)T (red symbols) along with the curves from model fitting (black solid lines). Within the probed temperature range from 25 °C to 77 °C, both sets of $I(Q)$ are seen to be in quantitative agreement with each other within experimental error when $Q > 0.03$ Å^{-1}. In both solutions, for $Q > 0.03$ Å^{-1} the incoherent backgrounds I_{inc} essentially show no dependence on temperature. Their magnitudes are found to be around 0.05 cm^{-1}. In the low Q region, the $I(Q)$ obtained from both solutions become discernibly different, and the magnitude of $I(Q)$ obtained from the P3(4MP)T solution is seen to be higher than that of the P3HT solution. Given that P3HT and P3(4MP)T have the same scattering length density due to their exact same chemical compositions and negligible inter-chain interactions at this dilute concentration, this observation reflects the difference in molecular weight between the two polymers.
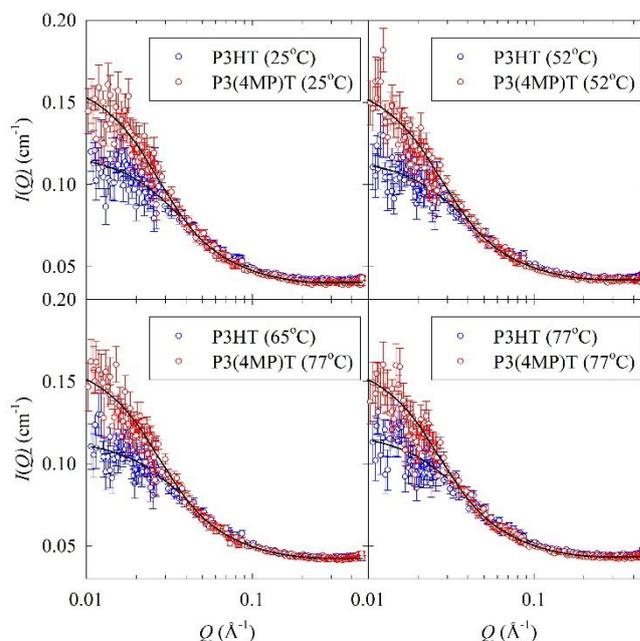
Figure 2. Comparison of the SANS absolute intensities $I(Q)$ obtained from the deuterated dichlorobenzene solutions of P3HT (blue symbols) and P3(4MP)T (red symbols) with a fixed concentration of 2 mg/mL at four different temperatures. Solid curves are the results of model fitting.

Having addressed the qualitative picture of the polymer conformations from the SANS spectra presented in Figures 1 and 2, one can further explore the structural details by examining the results from quantitative model fitting. In this study the SANS absolute intensity $I(Q)$ is modeled by the following expression:[42]

$$I(Q) = \frac{c}{N_A}\left(\frac{\Delta\rho}{d}\right)^2 M P_{SAC}(Q) R(Q) + I_{inc}, \quad (1)$$

where c is the weight fraction of conjugated polymers in solution, N_A is the Avogadro constant, $\Delta\rho$ is the difference in the bound scattering length density between polymer and solvent, d is the density of polymer, M is the molecular weight of a conjugated polymer chain, and I_{inc} is the incoherent scattering intensity, which is independent of Q. $R(Q)$ is the scattering function for the cross section of a cylinder with a radius of R_{CX} and is given by

$$R(Q) = \left[\frac{2J_1(QR_{CX})}{QR_{CX}}\right]^2, \quad (2)$$

where $J_1(x)$ denotes the Bessel function of the first kind. $P_{SAC}(Q)$ is the form factor of a conjugated polymer chain which describes the intra-chain spatial correlation. As demonstrated in Figure 1, the scattering behaviours of P3HT and P3(4MP)T are not in agreement with the prediction of the Debye model. To address the influence of excluded volume on a conjugated polymer coil, the scattering function for the form factor of a self-avoiding chain, $P_{SAC}(Q)$,[43] is used in this study. Building upon the phenomenological expression propose by Pedersen and Schurtenberger for the full scattering function of a single semiflexible chain[44] with excluded volume interactions, the improved scattering model by Chen et al. is used for model fitting and allows for the Kuhn length to be optimized. Model fitting allows quantitative structural information of the polymer chain to be obtained, including the chain contour length L, Kuhn length b, chain cross sectional radius R_{CX}, and chain radius of gyration R_G. Readers can refer to reference 43 for full numerical details of this model.
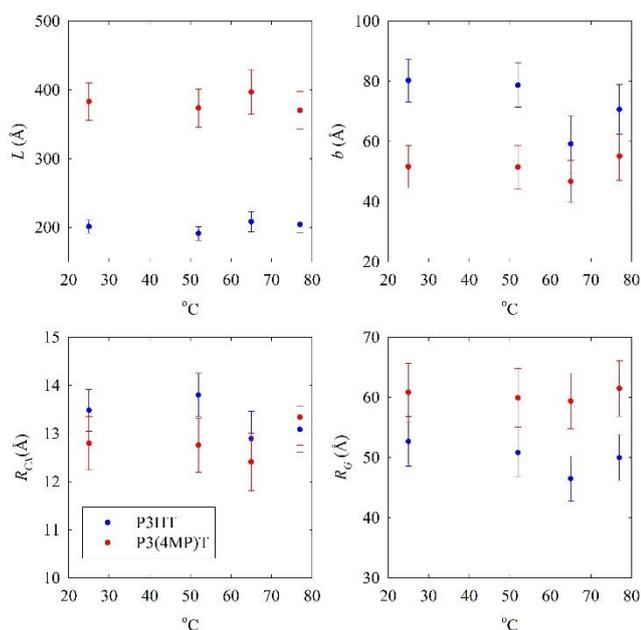
The results from model fitting are presented in Figure 3. Figure 3a presents the contour length L as a function of temperature. L is found to be around 200 Å and 370 Å for P3HT and P3(4MP)T, respectively, and both remain essentially unchanged within the probed temperature range. As indicated in Figure 2, the difference in $I(Q)$ observed in the low Q regime is due to the difference in M. Since $P_{SAC}(0) = 1$, Eqn. (1) shows that M can be calculated from the extrapolated zero-angle scattering intensity $I(0)$. From the chemical formula and density of d-DCB, the scattering length density (SLD) of d-DCB is 4.6 x 10^{-6} Å^{-2}. The scattering length density of P3HT has been measured[45] to be 0.676 x 10^{-6} Å^{-2}, corresponding to a density of approximately 1.15 g cm^{-3}, and because P3(4MP)T has the same chemical formula and is also likely to have a similar density to that of P3HT, it is assumed that the SLD of P3(4MP)T is also around 0.676 x 10^{-6} Å^{-2}. Thus, $\Delta\rho$ is calculated to be approximately -3.91 x 10^{-6} Å^{-2} for both P3HT and P3(4MP)T. Accordingly, SANS data analysis shows that M for P3HT and P3(4MP)T are 9.5 ± 0.3 kg/mol and 15.7 ± 0.3 kg/mol, respectively. Even though these results are lower than those determined by SEC, they more accurately represent the true molecular weight of the polymers, since SEC measured their apparent molecular weight based on their hydrodynamic volumes. Figure 3b shows results of the Kuhn length b, which describes the local stiffness of a conjugated polymer chain. P3HT appears to be more rigid than P3(4MP)T in d-DCB. Moreover, as demonstrated in Figure 3c, the cross section of a P3HT chain is seen to be almost identical to that of P3(4MP)T. The radius of gyration, R_G, has been commonly used to quantify the global size of a polymer chain. Due to the low signal-to-noise ratios in the low Q regime, extracting R_G from the Guinier approach[46] results in significant uncertainty. Alternatively, $P_{SAC}(Q)$ allows one to calculate the R_G of P3HT and P3(4MP)T from the corresponding L and b with satisfactory statistics, and the results are given in Figure 3d. As expected, R_G of P3(4MP)T is seen to be larger than that of P3HT due to the difference in molecular weight. Again, no discernible temperature dependence is observed.

Figure 3. Conformational characteristics of P3HT and P3(4MP)T as a function of temperature obtained from SANS model fitting: (a) contour length L; (b) Kuhn length b; (c) radius of chain cross section R_{CX}; and (d) radius of gyration R_G.
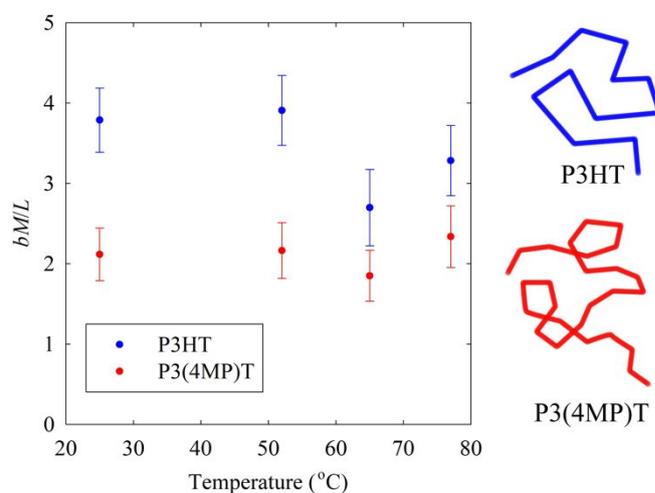
Figure 4. The ratio of bM/L for P3HT and P3(4MP)T as a function of temperature and the schematic representations of the global conformation of P3HT and P3(4MP)T, representing that P3(4MP)T is more flexible than P3HT.

To account for the difference in molecular weight between these two polymers, we normalize the Kuhn segment length *b* by the ratio of the chain contour length *L* to the chain molecular weight *M*, the results of which are shown in Figure 4. The ratio *bM/L* is found to be approximately between 3 - 4 for P3HT and about 2 for P3(4MP)T. As observed in the trend of Kuhn segment length *b* in Figure 3b, P3HT is clearly stiffer than P3(4MP)T. The origin of the observed difference in flexibility between P3HT and P3(4MP)T is a consequence of the different side chain chemistries. The backbone planarity of the chain influences the chain flexibility as well as the electronic conjugation. The branched side chain structure in P3(4MP)T possibly favours chain conformations that involve more twisting of the main chain as compared to P3HT with linear side chains. Therefore, P3HT is likely to have greater backbone planarity and, consequently, great chain stiffness, than P3(4MP)T.

It is instructive to compare our quantitative conformational characteristics with previous literature results. Aime et al. were the first to study the chain conformation of poly(3-alkylthiophenes) (P3ATs).[29,47] They determined the persistence length of poly(3-butylalkylthiophene) (P3BT) with a molecular weight of 49 kg/mol and Đ = 1.5 in nitrobenzene to be 27 Å by SANS. Heffner and Pearson used static light scattering and measured the persistence length of P3HT in the good solvent THF to be 24 ± 3 Å.[30] After synthetic techniques enabled the synthesis of regioregular polymers, Yamamoto et al. determined the persistence length of regioregular P3HT to be as high as 300 Å, suggesting a rather rigid conformation for P3HT.[32] More recently, the persistence length of regioregular P3HT dissolved in d-DCB was measured by Segalman and coworkers[36] to be approximately 30 Å at 40 °C, decreasing to approximately 15 - 20 Å at 160 °C, suggesting that P3HT adopts a semiflexible chain conformation. Zhang et al. developed a numerical and analytical approach for calculating the persistence length of complex semiflexible polymers, finding a persistence length of 32 Å for P3HT.[48] Nagai et al. investigated the effect of molecular weight on the conformational characteristics of P3HT, finding that the persistence length has considerable molecular weight dependence between 20 - 60 kg/mol, approaching a value of 30 Å at molecular weights larger than 60 kg/mol.[37] Our calculated R_G values of approximately 50 Å is consistent with the experimental R_G values measured by Nagai et al. (approximately 50 Å for P3HT with a molecular weight of 20 kg/mol). Model fitting results show that regioregular P3HT in d-DCB has a persistence length between 30 - 40 Å, discernibly larger than many of the aforementioned values reported in the literature. One possible reason for this discrepancy is the model selected for data analysis. Several theoretical scattering functions have been developed to address the conformation of a "*real*" polymer chain by incorporating the excluded volume effect into the Debye model. Among them is the phenomenological model developed by Sharp and Bloomfield,[49] which was used by Segalman and coworkers in their data analysis. However, computer simulations have demonstrated that this analytical model is only valid up to the spatial range of $Q^2 R_G^2 < 2$ and is therefore

unable to reliably resolve local structural details in a quantitative manner. Discussions about the limitation of the Sharp-Bloomfield model can be found elsewhere.[42,44] While a multitude of factors—including side chain chemistry, regioregularity, and synthetic route—can impact the chain persistence length, our results show that P3HT in a good solvent is a semiflexible chain with a persistence length of approximately 30 - 40 Å. By adding a branch point in the side chain, we observed that the persistence length decreases (chains become more flexible). This may be attributed to the branched side chain disfavouring the self-π-stacking interactions. Additionally, the branched side chain may also introduce steric restraints that lead to greater backbone torsion and, hence, a more flexible chain. Qualitatively, our results on the effect of side chain isomerism on P3AT chain flexibility are in agreement with Segalman et al., yet there are discrepancies in quantitative values due to our more accurate choice of SANS model.

In conclusion, we studied the conformation of poly(3-alkylthiophenes), a model conducting conjugated polymer system, dissolved in deuterated dicholorobenzene through small-angle neutron scattering. By examining the polymer chain flexibility, we demonstrate the profound impact of the spatial arrangement of side chain atoms on the backbone conformation. These results provide insight into the significant impact that topological isomerism can impart on conjugated polymer chain conformation, motivating future design of conjugated polymers with opportune π-π interactions, band gap, and hence, desirable optoelectronic properties.

Conflicts of interest

There are no conflicts to declare.

Acknowledgements

References

(1) Shirakawa, H.; Louis, E. J.; MacDiarmid, A. G.; Chiang, C. K.; Heeger, A. J. *Chem. Commun.* **1977**, 578.

(2) Handbook of Conducting Polymers, 3rd Ed. Edited by Skotheim, T. A.; Reynolds, J. CRC Press 2007.

(3) Sheiko, S. S.; Sumerlin, B. S.; Matyjaszewski, *K. Prog. Polym. Sci.* **2008**, *33*, 759.

(4) Inal, S.; Rivnay, J.; Suiu, A.-O.; Malliaras, G. G.; McCulloch, I. *Acc. Chem. Res.* **2018**, *51*, 1368.

(5) Heeger, A. J. *J. Phys. Chem. B.* **2001**, *105*, 8475.

(6) *Semiconducting Polymers: Applications, Properties, and Synthesis*, Edited by Hsieh, B.; Galvin, M.; Wei, Y., ACS Symp. Ser., Vol. 735, ACS, Washington DC, 1999.

(7) Wu, W.; Bazan, G. C.; Liu, B. *CHEM* **2017**, *2*, 760.

(8) Swager, T. M. *Angew. Chem. Int. Ed.* **2018**, *57*, 4248.

(9) Kuei, B.; Gomez, E. D. *Soft Matter* **2017**, *13*, 49.

(10) Minaev, B.; Baryshnikov, G.; Agren, H. *PCCP* **2014**, *16*, 1719.

(11) Wegmann, G. *et al.*, *PCCP* **1999**, *1*, 1795.

(12) For example, see Baker, G. L. In *Electronic and Photonic Applications of Polymers*, Edited by Bowden M. J.; Turner, S. R., Adv. Chem. Ser., Vol. 218, ACS, Washington DC, 1988.

(13) Olsen, B. D.; Segalman, R. A. *Mater. Sci. Eng. R.* **2008**, *62*, 37.

(14) Guo, Z. *et al.*, *PCCP* **2014**, *16*, 7764.

(15) He, Y.; Li, Y., *PCCP* **2011**, *13*, 1970.

(16) Mike, J. F. *et al.*, *PCCP* **2011***, 13*, 1338.

(17) Popere, B. *et al.*, *PCCP* **2012**, *14*, 4043.

(18) Pu, K.; Shuhendler, A. J.; Jokerst, J. V.; Mei, J.; Gambhir, S. S.; Bao, Z.; Rao, J. *Nat. Nanotechnol.* **2014**, *9*, 233.

(19) Smela, E. *Adv. Mater.* **2003**, *15*, 481.

(20) For example, see Dai, L. *J.M.S. Rev. Macromol. Chem. Phys.* **1999**, *C39*, 273.

(21) Mei, J.; Bao, Z. *Chem. Mater.* **2014**, *26*, 604.

(22) McCullough, R. D.; Tristram-Nagle, S.; Williams, S. P.; Lowe, R. D.; Jayaraman, M. *J. Am. Chem. Soc.* **1993**, *115*, 4910.

(23) Agbolaghi, S.; Zenoozi, S. *Org. Electron.* **2017**, *51*, 362.

(24) Snyder, C. R; Gomez, E. D. *J. Polym. Sci., Part B: Polym. Phys.* **2016**, *54*, 1202.

(25) Bombile, J. H.; Janik, M. J.; Milner, S. T. *PCCP* **2016**, *18*, 12521.

(26) Bombile, J. H.; Janik, M. J.; Milner, S. T. *PCCP* **2018**, *20*, 317.

(27) Teraoka, I. *Polymer Solutions: An Introduction to Physical Properties*, Wiley-Interscience: New York, 2002.

(28) Mueller, C. *et al.*, *Prog. Polym. Sci.* **2013**, *38*, 1978.

(29) Aime, J. P.; Bargain, F.; Schott, M.; Eckhardt, H.; Miller, G. G.; Elsenbaumer, R. L. *Phys. Rev. Lett.* **1989**, *62*, 55.

(30) Heffner, G. W.; Pearson, D. S. *Macromolecules* **1991**, *24*, 6295.

(31) Bi, X.; Ying, Q.; Qian, R. *Makromol. Chem.* **1992,** *193*, 2905.

(32) Yamamoto, T.; Komarudin, D.; Arai, M.; Lee, B. L.; Suganuma, H.; Asakawa, N.; Inoue, Y. Kubota, K.; Sasaki, S.; Fukuda, T.; Matsuda, H. *J. Am. Chem. Soc.* **1998**, *120*, 2047.

(33) Lecommandoux, S.; Chécot, F.; Borsali, R.; Schappacher, M.; Deffieux, A.; Brûlet, A.; Cotton, J. P. *Macromolecules* **2002**, *35*, 8878.

(34) Huang, Y.; Cheng, H.; Han, C. C. *Macromolecules* **2010**, *43*, 10031.

(35) Patel, S. N.; Javier, A. E.; Stone, G. M.; Mullin, S. A.; Balsara, N. P. *ACS Nano* **2012**, *6*, 1589.

(36) McCulloch, B.; Ho, V.; Hoarfrost, M.; Stanley, C.; Do, C.; Heller, W. T.; Segalman, R. A. *Macromolecules* **2013**, *46*, 1899.

(37) Nagai, M.; Huang, J.; Zhou, T.; Huang, W. *J. Polym. Sci., Part B: Polym. Phys.* **2017**, *55*, 1273.

(38) Tamba, S.; Tanaka, S.; Okubo, Y.; Meguro, H.; Okamoto, S.; Mori, A. *Chem. Lett.* **2011**, *40*, 398.

(39) Mercier, L. G.; Leclerc, M. *Acc. Chem. Res.* **2013**, *46*, 1597.

(40) Tamao, K; Sumitani, K; Kumada, M. *J. Am. Chem. Soc.* **1972**, *94*, 4374.

(41) Debye, P. *J. Phys. Colloid Chem.* **1947**, *51*, 18.

(42) Schurtenberger, P. In *Neutron, X-rays and Light. Scattering Methods Applied to Soft Condensed Matter*, Edited by Lindner, P.; Zemb, Th.; North-Holland: Amsterdam, 2002.

(43) Chen, W.-R.; Butler, P. D.; Magid, L. J. *Langmuir* **2006**, *22*, 6539.

(44) Pedersen, J. S.; Schurtenberger, P. *Macromolecules* **1996**, *29*, 7602.

(45) Newbloom, G. M.; Weigandt, K. M.; Pozzo, D. C. *Soft Matter* **2012**, *8*, 8854.

(46) Guinier, A.; Fourmet, G. *Small-Angle Scattering of X-rays*, John Wiley and Sons: New York 1955.

(47) Aime, J.P.; Bargain, F.; Schott, M.; Eckhardt, H.; Elsenbaumer, R.L.; Miller, G.G.; McDonnell, M.E.; Zero, K. *Synth. Met.* **1989**, *28*, C407.

(48) Zhang, W.; Gomez, E. D.; Milner, S. T. *Macromolecules* **2014**, *47*, 6453.

(49) Sharp, P.; Bloomfield, V. A. *Biopolymers* **1968**, *6*, 1201.